CHAPTER 6

DENSITY FUNCTIONAL STUDY OF MAGNETIC PARAMETERS IN $(NiO)_n$ NANOCLUSTERS

INTRODUCTION

Nanoscale transition metal clusters have found wide-range of applications in catalysis, energy conversion, electronics, etc. Nickel oxides are one of those very important metal clusters which have found chemical and metallurgical grade specialized applications. Nickel oxides have been widely used for electrochromic anodes for the last decades. Functionalities like optical and magnetic properties, molecular trapping and thermal response have been exhibited by these clusters. The small size and their well dispersive property make them desirable for many applications in magnetic, electrochromic, chemisorptions, ceramic and heterogeneous catalysis [1,2]. The reason that these types of nanoclusters are in high demand in every field is that they exhibit different chemical and physical properties as compared to the bulk phases. Another advantage of such metal clusters is that they can be tuned as our requirement. Hence the synthesis and characterization of nanoclusters is very important. Various sizes of such nanoclusters and their respective structural changes lead to the discovery of new materials with advantageous properties [3]. An attempt to exploit the desirable requirements, the possible geometries of such transition metal clusters are necessary to be studied along with their properties. Experimentally the particle size and geometries are designed by varying the relative rates of nucleation and cluster growth but theoretically the most probable and stable nanocluster geometries are looked-for which are actually computationally expensive. Hence in this study we have tried to obtain possible geometries of Ni_nO_n (where n=2 to 7) series of clusters and to correlate them with their respective ZFS parameters.

Since the derivation of structural information of such nanoclusters, from experimental details are difficult, hence computational simulations are frequently used for the prediction of their properties. One of such new and significant programs is Knowledge Led Master Code (KLMC) [4] which we have used in our case to obtain the predictable geometries of the nickel oxides.

6.1. Theory

The KLMC program can automate various tasks traditionally performed by hand. The algorithms used by the in-built KLMC package have employed standard local optimization methods to relax trial random atomic configurations which are initially designed to improve convergence to local energy minima. A global optimization run is done in order to find the stable configurations of the $(NiO)_n$ series of nanoclusters. The method of locating the local energy minimum is stated as minimum or basin hopping [5−7] EPR studies of transition metal systems were successfully done earlier wherein it is showed that the theoretical magnetic parameters give fruitful values when compared to the experimental results [8−10] Hence we have also tried to calculate the EPR parameters D-tensor as well as g-tensor.

The g-tensor for transition metal complexes is actually a correction for the g-value of free electron i.e.,

$$g = g_e 1 + \Delta g$$

where g_e = 2.002319. Calculation of the g-tensor involves second-order perturbation theory which includes the relativistic mass-correction term, the diamagnetic spin-orbit and the paramagnetic spin-orbit term respectively. We can say that the g-shift consists of the relevant Breit-Pauli terms:

$$\Delta g = \Delta g_{SO/OZ} + \Delta g_{RMC} + \Delta g_{GC}$$

The first term pairs up the perturbation due to the field-independent spin-orbit operators (SO) and the orbital Zeeman interaction (OZ), second refers to relativistic mass correction term while the third term stands for gauge-correction.

The ZFS describes the removal of the state degeneracy for systems with S>1/2 in absence of magnetic field. By choosing a coordinate system that diagonalizes D, we can express H_{ZFS} as:

$$H_{ZFS} = D\left[s_z^2 - \frac{1}{3}S(S+1)\right] + E(s_x^2 - s_y^2$$

$$D = D_{zz} - \frac{1}{2}(D_{xx} - D_{yy})$$

Here, D and E are axial and rhombic ZFSs.

6.2 Computational Details

First of all the $(NiO)_n$ nanocluster series from n=2−7 are pre-screened in KLMC. The KLMC generated geometries were further considered for re-optimization and refined at DFT level. KMLC calls FHI-aims and their respective total energies are calculated. For the optimized geometries of these nickel oxide clusters, by default “light” settings were employed which is analogous with split valence and double zeta basis sets used in usual Gaussian codes. In addition to this, grids with a scalar ZORA relativistic treatment [11] are employed. During relaxations, the relax_geometry with the bfgs algorithm is used to obtain reliable structure optimizations. GGA exchange-correlation functional PBE is used. Moreover for Ni, being a heavy element, “tier 1” is sufficient for tightly converged ground state properties, where tier 1 being analogous to ‘double numeric plus polarization’ basis set in literature.

Considering the geometries from FHI-AIMS package [12,13], the magnetic parameters g-tensor and D-tensor were studied by employing single point calculation in the ORCAprogram package [14]. For the Ni atoms we have used the Stuttgart/Dresden ECPs (SDD) [15] basis sets and the def2-TZVP [16,17] Ahlrichs basis set for Coulomb fitting, i.e. def2-TZVP/J [18] is used. For the O atoms def2-TZVP basis set is used. The functional used is B3LYP [19] functional. For transition metal complexes for which the relativistic effects are significant the spin-orbit contributions for D-tensors and the g-tensors are calculated via the spin-orbit mean-field (SOMF) approach [20]. Besides this approach, the spin-orbit contribution to the total D-value is calculated by using the Coupled Perturbed (CP) method [21]. The CP method solves a set of coupled-perturbed equations for the SOC perturbation. There are many instances in literature where CP method is being found to be the most effective in calculation of ZFS parameter as well as in estimation of spin-orbit contribution towards the total D-value [22−24]. In our case we have studied the EPR properties for the Ni nuclei using the flags for the calculation of the isotropic part, dipolar part, second-order contribution to g-tensor from SOC and electric field gradient fraction. For calculation of EPR parameters, the spin unrestricted technique is preferably used, because it can account for experimentally observed phenomena such as negative spin density [25].

6.3 Results and discussion

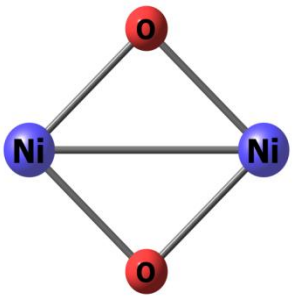

Ni_2O_2

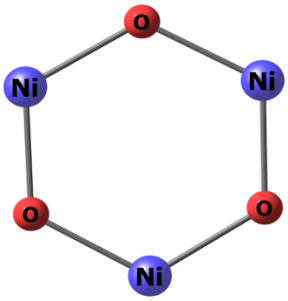

Ni_3O_3

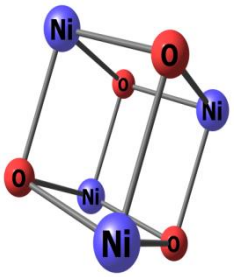

Ni_4O_4_first

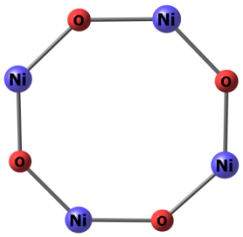

Ni_4O_4_second

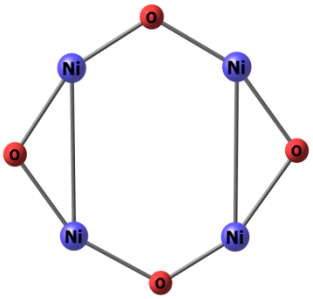

Ni4O_4_third

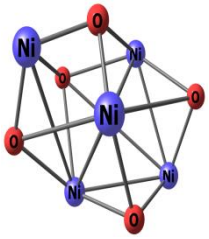

Ni_5O_5_first

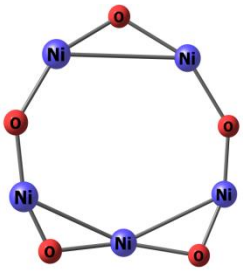

Ni_5O_5_second

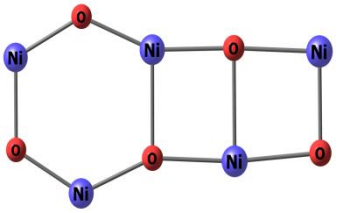

Ni_5O_5_third

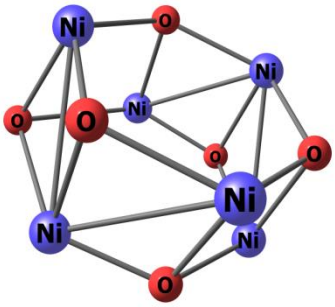

Ni_6O_6_first

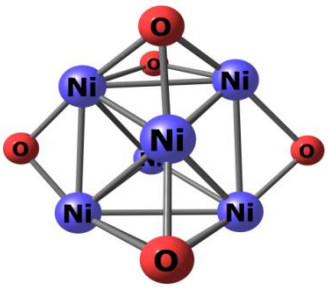

Ni_6O_6_second

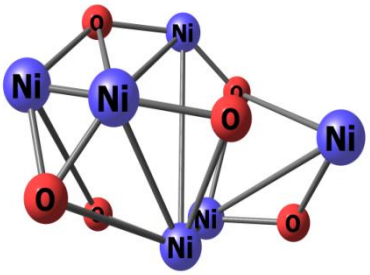

Ni_6O_6_third

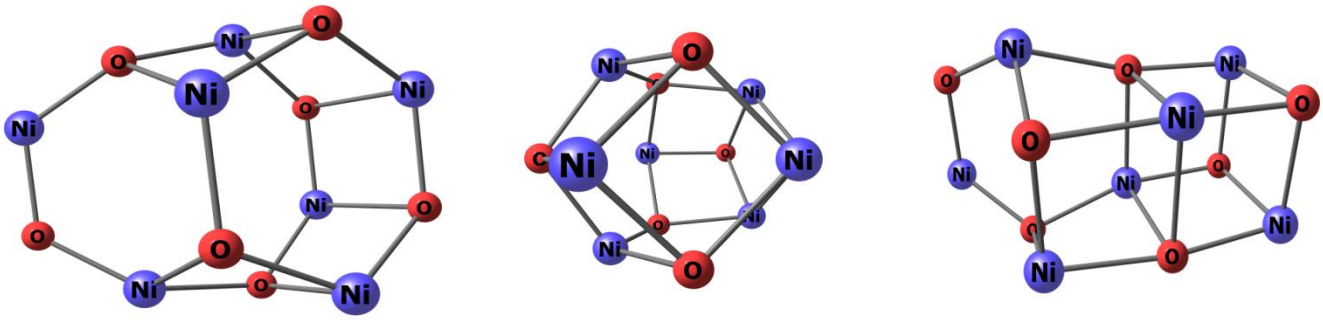

Ni_7O_7_first Ni_7O_7_second Ni_7O_7_third

Figure 6.1: Optimized geometries of $(NiO)_n$ series (where n=2 to 7)

The optimized geometries of $(NiO)_n$ nanoclusters are shown in the Figure 6.1. The figures are positioned in the order of KLMC generated energy sequence as first, second and third (first being the most stable). $(NiO)_2$ and $(NiO)_3$ have only single possible lowest energy geometries unlike the rest, i.e., $(NiO)_n$ for n=4–7 whose three lowest-energy structures we have taken for consideration. Taking into account the most stable structural isomers, their second energy differences are plotted as shown in Figure 6.2. Generally the stability of metal clusters is studied by plotting second energy difference which is mathematically calculated as:

$$\Delta_2 E_n^* = 2E_n^* - (E_{n-1}^* + E_{n+1}^*)$$

where$E_n^* = E_n - nE_1$which is PBE energy difference. We know that $\Delta_2 E_n^*$ is the relative binding energy [26] of a $(NiO)_n$ cluster with respect to $(NiO)_{n+1}$ and $(NiO)_{n-1}$ clusters. Therefore, peaks in Figure 6.2 represents relatively more stable clusters. Thus, the second energy difference shows the relative change in energy of the nanoclusters with respect to n. From n=2–7, here appears one minima and one maxima.

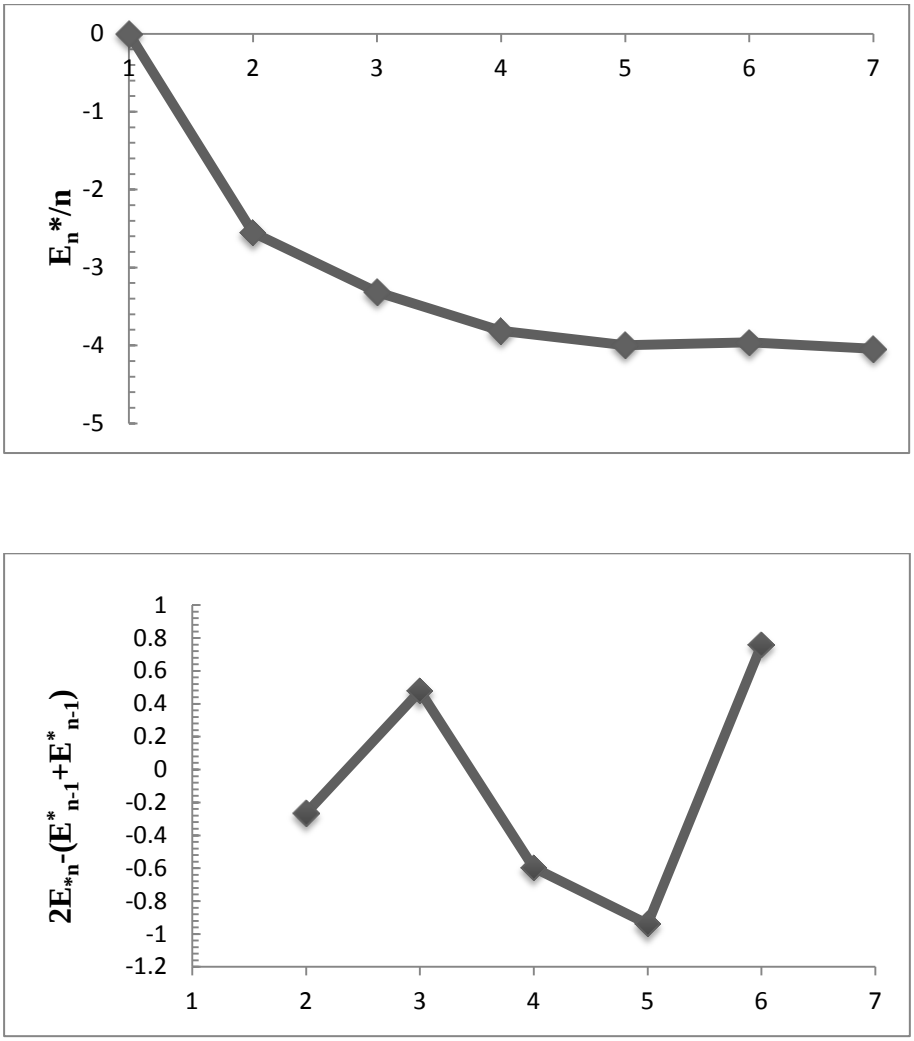

Figure 6.2: PBE energy difference, $E_n^* = E_n - nE_1$, and the second energy difference of $(NiO)_n$ nanoclusters

Table 6.1: Table showing FHI-AIMS generated energies for the $(NiO)_n$ series (where n=2 to 7)

Cluster	Energies (in eV)	(in Hartree)
Ni_2O_2	-87221.353	**-3205.371**
Ni_3O_3	-130834.316	**-4808.140**
Ni_4O_4_first	-174447.708	**-6410.926**
Ni_4O_4_second	-174446.844	**-6410.894**
Ni_4O_4_third	-174447.756	**-6410.927**
Ni_5O_5_first	-218058.403	**-8013.612**
Ni_5O_5_second	-218060.600	**-8013.693**
Ni_5O_5_third	-218060.600	**-8013.692**
Ni_6O_6_first	-261670.710	**-9616.357**
Ni_6O_6_second	-261672.179	**-9616.411**
Ni_6O_6_third	-261672.505	**-9616.423**
Ni_7O_7_first	-305063.868	**-11217.049**
Ni_7O_7_second	-305285.091	**-11219.179**
Ni_7O_7_third	-305285.169	**-11219.182**

FHI-AIMS re-optimizes the possible structures of these $(NiO)_n$ clusters pre-screened by the KLMC program, and calculate their energies which is tabulated as in Table 6.1. It is noteworthy from the Table above that the sequence of the stable geometries pre-screened by KLMC (as first, second and third) and the sequence obtained from the FHI-AIMS program do not match in order. Besides this, the refined structural parameters of $(NiO)_n$ nanoclusters of the geometries generated by FHI-AIMS code also differs from that of the KLMC generated geometries.

Table 6.2: Table showing EPR parameters g-tensor and D-tensor for the $(NiO)_n$ series (where n=2 to 7)

Cluster	g-Tensor			g_{iso}	D-tensor (in cm^{-1})
Ni_2O_2	1.786	1.815	2.031	1.878	59.063
Ni_3O_3	1.968	2.180	2.184	2.111	50.893
Ni_4O_4_first	1.994	2.077	2.155	2.076	28.804
Ni_4O_4_second	1.730	2.126	2.453	2.103	84.527
Ni_4O_4_third	1.955	2.124	2.245	2.108	109.181
Ni_5O_5_first	1.976	2.161	2.209	2.116	-39.801
Ni_5O_5_second	1.796	2.150	2.295	2.080	-43.310
Ni_5O_5_third	1.848	2.195	2.285	2.109	53.952
Ni_6O_6_first	2.032	2.116	2.147	2.098	16.309
Ni_6O_6_second	2.004	2.047	2.304	2.118	105.268
Ni_6O_6_third	1.970	2.031	2.297	2.099	75.509
Ni_7O_7_first	1.991	2.037	2.047	2.025	-9.397
Ni_7O_7_second	1.986	2.086	2.233	2.102	40.561
Ni_7O_7_third	1.958	2.146	2.266	2.124	-71.393

Table 6.2 reports the D-tensor as well the g-tensor values of the $(NiO)_n$ nanoclusters calculated theoretically from the ORCA program package. The clusters are verified to be in triplet state as yielded by the quasi-restricted MO's. The g-tensors of the clusters have shown significant deviation from the g-value of free electron which is 2.0023. Hence the general inference from this result is that these nickel oxide clusters exhibit considerable quantity of magnetic anisotropy. Such significant amount of magnetic anisotropy is explained due to magnetic field-induced coupling between the metal and the oxygen atom orbitals. Such a large deviation from the g-value of free electron implies notable spin-orbit angular momentum between the Ni and the O atoms, which is similar as in the

case of ligand field theory pertinent to metal complexes. According to Mulliken gross atomic population calculation, approximately 70% of the charge is localized on the Ni atoms and hence larger contribution to g-tensor comes from the spin-orbit coupled with orbital Zeeman effect $\Delta g_{SO/OZ}$. This shows enhanced contribution from the metal orbitals and this gives rise to *g*-anisotropy.

The D-tensor values for the clusters have shown to have positive values in most of the cases.Most of the clusters are speculative of having positive D-values. However, it is well established that negative axial anisotropy is a consequential criterion for a system to exhibit effective single molecule magnetic behaviour. Besides, respective disparity between covalencies (the orbital reduction factors) is a cause for negative D-value. Hence one can construe that those clusters having positive D-values have insignificant covalencies and charge separation between the metal and the O atoms. For two of the $(NiO)_5$ and $(NiO)_7$ clusters negative sign of D-tensor asserts their single molecular magnetic behaviour. There occurs relaxation of magnetization at low temperature for single molecule magnets (SMMs), because there is an energy barrier to loss of magnetization due to negative D-tensor of the spin ground state S. This further removes the degeneracy of the $M_s$spin triplet states, and since D is negative, M_s=0 is highest in energy at zero-field, while M_s=±1 are lowest in energy, with the former at an energy of $|D|S_z^2$ with respect to the later. On the other hand, positive D-tensor corresponds to non-magnetic M_s=0 state at ground state. Depending on the sign, the magnetization is aligned along an easy axis (negative D) or within an easy plane (positive D). Moreover, the clusters being multinuclear, exhibit magnetic superexchange through the correlated O orbitals which is further facilitated by Coulomb exchange on the oxygen. This is observed from the exchange contribution as calculated along with the D-tensor. Hence some D-values are as high as ~100 cm^{-1}.

This zero-field splitting (ZFS) parameter D-tensor has the following as the key features contributing towards the total D-tensor, they are: spin-orbit coupling (D_{SOC}) as well as spin-spin coupling (D_{SS}). The splitting of the overall D-tensor into the spin-spin (D_{SS}) and spin-orbit coupling (D_{SOC}) components is shown in Table 6.3.

Table 6.3: Contribution of spin-spin and spin-orbit coupling towards total D-tensor for the $(NiO)_n$ series (where n=2 to 7)

Cluster	***D-tensor*** **(in cm^{-1})**	D_{SS} **(in cm^{-1})**	D_{SOC} **(in cm^{-1})**	***E/D***
Ni_2O_2	59.063	1.001	58.142	0.018
Ni_3O_3	50.893	1.936	48.918	0.043
Ni_4O_4_first	28.804	0.343	28.222	0.018
Ni_4O_4_second	84.527	5.749	78.778	0.118
Ni_4O_4_third	109.181	3.387	105.714	0.081
Ni_5O_5_first	-39.801	-0.573	-39.065	0.204
Ni_5O_5_second	-43.310	2.758	-45.926	0.243
Ni_5O_5_third	53.952	0.595	51.738	0.285
Ni_6O_6_first	16.309	0.963	14.872	0.248
Ni_6O_6_second	105.268	1.329	103.833	0.097
Ni_6O_6_third	75.50983	2.616	73.013	0.173
Ni_7O_7_first	-9.397	0.089	-9.474	0.166
Ni_7O_7_second	40.561	-0.749	41.914	0.236
Ni_7O_7_third	-71.393	-2.837	-67.617	0.252

Usually it is seen in transition metal complexes that where the D-tensor values are smaller, the contribution from spin-spin part is overestimated and quantitatively significant with ~30% contribution [24,27]. However, in case of this series of nickel oxide clusters, the contribution from the spin-spin coupling towards the total D-tensor is negligible which varies from 1 to 6%. Therefore, in this case, the spin-spin part is expected to bring trivial benefaction to the overall anisotropy.

It is considered that four types of excitations contribute to the D_{SOC} part. These excitations include same-spin, α→α (SOMO→VMO) and β→β (DOMO→SOMO) excitations, where α and β are spin-up and spin-down electrons respectively; and the

other two excitations are spin-flip excitations, i.e., α→β (SOMO→SOMO) and β→α (DOMO→VMO). All these four types of excitations, in this series of $(NiO)_n$ clusters, are shown in Table 6.4.

Table 6.4: Decomposed values of D_{SOC} for the $(NiO)_n$ series (where n=2 to 7) obtained from CP method

Cluster	D_{SOC} (in cm^{-1})	Decomposition of D_{SOC}			
		SOMO→VMO α→α (in cm^{-1})	DOMO→SOMO β→β (in cm^{-1})	SOMO→SOMO α→β (in cm^{-1})	DOMO→VMO β→α (in cm^{-1})
Ni_2O_2	58.142	4.569	6.542	40.927	6.103
Ni_3O_3	48.918	9.814	-10.133	53.489	-4.252
Ni_4O_4_first	28.222	17.88	-6.605	23.455	-6.508
Ni_4O_4_second	78.778	51.626	-47.891	95.443	-20.4
Ni_4O_4_third	105.714	24.207	-13.347	103.824	-8.97
Ni_5O_5_first	-39.065	-8.121	25.695	-58.474	1.834
Ni_5O_5_second	-45.926	-46.732	46.058	-50.236	4.983
Ni_5O_5_third	51.738	6.477	-6.974	57.77	-5.536
Ni_6O_6_first	14.872	7.39	-1.453	9.11	-0.175
Ni_6O_6_second	103.833	34.692	-20.527	103.711	-14.043
Ni_6O_6_third	73.013	15.602	-35.881	99.895	-6.603
Ni_7O_7_first	-9.474	-3.586	4.384	-12.04	1.767
Ni_7O_7_second	41.914	22.83	-11.38	38.306	-7.842
Ni_7O_7_third	-67.617	-28.288	16.402	-68.526	12.796

It is observed that the highest contribution comes from the spin-flip α→β excitation between two singly occupied MO (SOMO) that leads to states of S´=S-1. This excitation couples the excited states if an *S─1* total multiplicity to the ground state.

We have investigated the geometry and their respective stability of $(NiO)_n$ (where n=2–7) nanoclusters using the KLMC program to locate the DFT energy minima and then to get the optimized geometries employing the FHI-aims package. Their corresponding magnetic properties, D-tensor and g-tensor were calculated in the ORCA program package. The g-tensor values of these nanoclusters are appreciably deviating from that of the free electron values and this connotes significant magnetic anisotropy. On the other hand the D-tensor values for most of them are observed to have positive sign which testifies that they are not suitable to be used as single molecule magnets. Also the D-values are fairly high and this can be attributed to the existence of superexchange between Ni atoms via the bridging O atoms. The overall D-tensor is a result of spin-spin and spin-orbit coupling contribution and in this case the spin-spin contribution is very trivial unlike in coordinate metal complexes.

REFERENCES

[1] Tao, D. and Wei, F. New procedure towards size-homogeneous and well-dispersed nickel oxide nanoparticles of 30 nm. *Materials Letters*, 58(25):3226–3228, 2004.

[2] Wang, Y., Zhu, J., Yang, X., Lu, L. and Wang, X. Preparation of NiO nanoparticles and their catalytic activity in the thermal decomposition of ammonium perchlorate. *Thermochimica Acta*, 437(1-2):106–109, 2005.

[3] Woodley, S. M. and Catlow, R. Crystal structure prediction from first principles. *Nature materials*, 7(12):937, 2008.

[4] Woodley, S. M. Knowledge Led Master Code search for atomic and electronic structures of LaF_3 nanoclusters on hybrid rigid ion-shell model-DFT landscapes. *The Journal of Physical Chemistry C*, 117(45):24003–24014, 2013.

[5] Cheng, L., Feng, Y., Yang, J., and Yang, J. Funnel hopping: Searching the cluster potential energy surface over the funnels. *The Journal of Chemical Physics*, 130(21):214112, 2009.

[6] Goedecker, S. Minima hopping: An efficient search method for the global minimum of the potential energy surface of complex molecular systems. *The Journal of chemical physics*, 120(21):9911–9917, 2004.

[7] Wales, D. J. and Doye, J. P. Global optimization by basin-hopping and the lowest energy structures of Lennard-Jones clusters containing up to 110 atoms. *The Journal of Physical Chemistry A*, 101(28):5111–5116, 1997.

[8] Neese, F. Importance of direct spin-spin coupling and spin-flip excitations for the zero-field splittings of transition metal complexes: A case study. *Journal of the American Chemical Society*, 128(31):10213–10222, 2006.

[9] Gómez-Coca, S., Aravena, D., Morales, R. and Ruiz, E. Large magnetic anisotropy in mononuclear metal complexes. *Coordination Chemistry Reviews*, 289:379–392, 2015.

[10] Boča, R. Zero-field splitting in metal complexes. *Coordination Chemistry Reviews*, 248(9-10):757–815, 2004.

[11] van Lenthe, E., Baerends, E. J. and Snijders, J. G. Relativistic total energy using regular approximations. *The Journal of Chemical Physics*, 101(11):9783–9792, 1994.

[12] Havu, V., Blum, V., Havu, P. and Scheffler, M. Efficient O (N) integration for all-electron electronic structure calculation using numeric basis functions. *Journal of Computational Physics*, 228(22):8367–8379, 2009.

[13] Blum, V., Gehrke, R., Hanke, F., Havu, P., Havu, V., Ren, X. and Scheffler, M. *Ab initio* molecular simulations with numeric atom-centered orbitals. *Computer Physics Communications*, 180(11):2175–2196, 2009.

[14] Neese, F., Wennmohs, F., Becker, U., Bykov, D., Ganyushin, D., Hansen, A. and Pantazis, D. A. *ORCA, version 3.0.* Institute for physical and theoretical chemistry, Bonn, 2014.

[15] Andrae, D., Haeussermann, U., Dolg, M., Stoll, H. and Preuss, H. Energy-adjusted ab initio pseudopotentials for the second and third row transition elements. *Theoretica Chimica Acta*, 77(2):123–141, 1990.

[16] Goerigk, L., Moellmann, J. and Grimme, S. Computation of accurate excitation energies for large organic molecules with double-hybrid density functionals. *Physical Chemistry Chemical Physics*, 11(22):4611–4620, 2009.

[17] Schäfer, A., Huber, C. and Ahlrichs, R. Fully optimized contracted Gaussian basis sets of triple zeta valence quality for atoms Li to Kr. *The Journal of Chemical Physics*, 100(8):5829–5835, 1994.

[18] Weigend, F. Accurate Coulomb-fitting basis sets for H to Rn. *Physical Chemistry Chemical Physics*, 8(9):1057–1065, 2006.

[19] Becke, A. D. Density-functional thermochemistry. III. The role of exact exchange. *The Journal of Chemical Physics*, 98(7):5648–5652, 1993.

[20] Heß, B. A., Marian, C. M., Wahlgren, U. and Gropen, O. A mean-field spin-orbit method applicable to correlated wavefunctions. *Chemical Physics Letters*, 251(5-6):365–371, 1996.

[21] Neese, F. Metal and ligand hyperfine couplings in transition metal complexes: The effect of spin–orbit coupling as studied by coupled perturbed Kohn-Sham theory. *The Journal of Chemical Physics*, 118(9):3939–3948, 2003.

[22] Zein, S. and Neese, F. Ab initio and coupled-perturbed density functional theory estimation of zero-field splittings in Mn(II) transition metal complexes. *The Journal of Physical Chemistry A*, 112(34):7976–7983, 2008.

[23] Neese, F. Prediction of electron paramagnetic resonance g values using coupled perturbed Hartree-Fock and Kohn-Sham theory. *The Journal of Chemical Physics*, 115(24):11080–11096, 2001.

[24] Dutta, S. and Deka, R. C. Zero field splitting in Mn (III) complexes: A comparative study of DFT base Coupled-Perturbed and Pederson–Khanna approaches. *Computational and Theoretical Chemistry*, 1072:1–6, 2015.

[25] Wertz, J. E. and Bolton, J. R. *Electron Spin Resonance Spectroscopy*. Chapman and Hall, New York, 1986.

[26] Harbola, M. K. Magic numbers for metallic clusters and the principle of maximum hardness. Proceedings of the National Academy of Sciences, 89(3):1036–1039, 1992.

[27] Zein, S., Duboc, C., Lubitz, W. and Neese, F. A systematic density functional study of the zero-field splitting in Mn (II) coordination compounds. *Inorganic Chemistry*, 47(1):134–142, 2008.